Continuum description of rarefied gas dynamics. III. The structures of shock waves

Xinzhong Chen and Edward A. Spiegel
Astronomy Department, Columbia University, New York, New York 10027

Hongling Rao
Microeletronics Sciences Laboratories, Columbia University, New York, New York 10027

(Received 21 May 2001; revised manuscript received 6 August 2001; published 12 February 2002)

We use the one-dimensional steady version of the equations derived in paper I to compute the structure of shock waves and find good agreement with experiment.

DOI: 10.1103/PhysRevE.65.036304 PACS number(s): 05.20.Dd, 47.45.−n, 51.10.+y, 51.20.+d

I. INTRODUCTION

In the simplest description of a shock wave, one uses the Euler equations of fluid dynamics to develop jump conditions across the discontinuity that describes the shock. These conditions have qualitative value but there are problems for which such limiting solutions are not adequate. For example, in studying radiation from shock waves, say, to infer the properties of the radiating atoms, the conditions within the shocks may become important. If the matter ahead of the shock is neutral and that behind the shock is fully ionized, the observed spectral lines may be formed within the shock itself and so conditions there need to be carefully worked out. This example is one of many that we might have cited to motivate our present study of the structure of shock waves. Even a cursory look at the literature on this problem gives a clear picture of the importance that has been attached to it.

Much of the work on the structure of shock waves has been aimed at improving the description provided by the Navier-Stokes equations. A review of such attempts was given by Galkin and Shavaliev [1], who compared various higher order solutions of the Boltzmann equation with results from the Chapman-Enskog [2] and Hilbert methods [3]. In terms of shock structure alone, the higher order solutions give a significantly improved result [4,5], but a number of fundamental problems concerning the status of these equations remain open [1,3,6,7]. It is especially troubling that a large number of higher order nonlinear terms in some of the proposed improvements make it difficult to use the results in realistic problems. Similar difficulties beset extensions of Grad's moment method [3,8], such as the extended irreversible thermodynamics (EIT) [9], which does give good results for the problem of ultrasonic sound wave propagation. It remains true, however, that a large number of equations must be solved to achieve reasonable accuracy with EIT.

When the densities are sufficiently low, direct numerical simulation by the Monte Carlo method is the most reliable way in which to compute high-Knudsen-number flows, although the computational cost may be high in regimes near continuum limits [10]. In the case of the relaxation (or BGKW) model, which is formally linear, the formal solution of that problem may be used and this approach has worked well in two-dimensional problems [11]. Nevertheless, an effective macroscopic description would be of value for problems in which the Knudsen number is not infinitesimal. In this article, we intend to show how the equations derived in paper I [12] may fill this need. To do this, we work out the structure of shock waves in one-dimensional steady flow starting from the equations of paper I. Those equations were derived from kinetic theory without using some of the traditional simplifications associated with the Chapman–Enskog approach. In particular, we did not use results from lower order approximations to simplify higher order equations. In paper II [13], the first-order development (in the mean free path) of paper I was tested against observations of ultrasound propagation.

In the present article, we go on to see how well the theory works for the computation of the structure of shock waves. Since the shock thickness is typically of the order of a mean free path, we are pushing against the formal limits of validity of the expansions used in deriving fluid equations. We confront in addition the challenge of strong nonlinearity. Moerover the flow considered in shock theory is far from thermodynamic equilibrium, so this too makes for a stringent test.

A simplification that makes comparisons relatively easy to draw is that, in the study of shocks, we may separate the continuum differential equations of fluid motion from the boundary conditions that must be stated to complete a well-posed problem. The boundary conditions for the shock problem are not at issue since we may impose the jump conditions given above, reexpressed as Rankine-Hugoniot relations, to serve the role of the boundary conditions. Hence in this study of shock structure, we are able to focus on effects due only to the differential equations themselves and in doing so examine the validity of our version of the fluid equations.

In Sec. II, we recall the fluid dynamical equations derived in paper I. In Sec. III, we rearrange the equations to facilitate the calculation of the shock structure. Then, in Sec. IV, the structures of one-dimensional shock waves computed with these equations are compared to analogous results obtained with the Navier-Stokes equations as well as with experiments. We conclude with a brief summary in Sec. V.

II. STATEMENT OF THE EQUATIONS

In paper I we proposed a modification of the usual asymptotic techniques for deriving fluid equations from kinetic theory. Our procedure avoids the simplification intro-

duced by Chapman and Enskog [2] in which the results of lower approximations are introduced into the higher approximations. When we proceed in this way, we obtain these fluid equations [12–15]:

$$\partial_t \rho + \boldsymbol{\nabla}\cdot(\boldsymbol{\rho}\mathbf{u}) = 0, \tag{2.1}$$

$$\partial_t u + \mathbf{u}\cdot\nabla\mathbf{u} + \frac{1}{\rho}\boldsymbol{\nabla}\cdot\mathsf{P} = 0, \tag{2.2}$$

$$\partial_t T + \mathbf{u}\cdot\boldsymbol{\nabla}T + \frac{2}{3\rho R}(\mathsf{P}:\boldsymbol{\nabla}\mathbf{u} + \boldsymbol{\nabla}\cdot\mathbf{Q}) = 0, \tag{2.3}$$

where ρ is the mass density, $\mathbf{u}$ is the average velocity of the particles in a fluid element cell, and T is the temperature. We assume that the gas is made up of identical, structureless particles with mass m so that $R=k/m$ is the gas constant with k the Boltzmann constant. Our expression for the stress tensor is

$$\mathsf{P} = \left[\rho RT - \mu\left(\frac{D\ln T}{Dt} + \frac{2}{3}\boldsymbol{\nabla}\cdot\mathbf{u}\right)\right]\mathsf{I} - \mu\mathsf{E}:\boldsymbol{\nabla}\boldsymbol{\nabla}\mathbf{u}, \tag{2.4}$$

where

$$\frac{D}{Dt} = \partial_t + \mathbf{u}\cdot\boldsymbol{\nabla}, \tag{2.5}$$

and

$$\mu = \tau\rho RT \tag{2.6}$$

is the viscosity expressed in terms of the mean free time τ. For the shear stress tensor we have the usual expression,

$$E^{ij} = \frac{\partial u^i}{\partial x_j} + \frac{\partial u^j}{\partial x_i} - \frac{2}{3}\boldsymbol{\nabla}\cdot\mathbf{u}\delta^{ij}. \tag{2.7}$$

Finally, for the heat current, we have

$$\mathbf{Q} = -\eta\nabla\ln(\rho T^{-(3/2)}) - \frac{7}{2}\eta\boldsymbol{\nabla}\ln T - \frac{5}{2}\mu\frac{D\mathbf{u}}{\mathbf{Dt}}, \tag{2.8}$$

where $\eta = \frac{5}{2}\mu RT$ for the relaxation model.

By contrast, in the Navier-Stokes equations with no bulk viscosity, one has

$$\mathsf{P} = \rho RT\mathsf{I} - \mu\mathsf{E}:\boldsymbol{\nabla}\boldsymbol{\nabla}\mathbf{u} \tag{2.9}$$

and

$$\mathbf{Q} = -\eta\boldsymbol{\nabla}\ln T. \tag{2.10}$$

III. SHOCK THEORY

A. Basic equations

As indicated in Fig. 1, when the velocity of the flow in the upstream ($x\to-\infty$) exceeds the sound speed of the medium, a shock front forms. In a frame comoving with the front, a steady shock layer forms. Its structure is determined by the upstream thermodynamic quantities and the dissipation mechanism. The form of the shock wave provides a straightforward test of the equations.

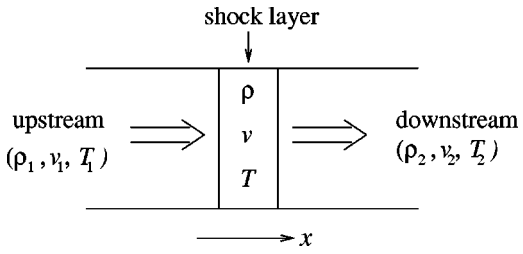

FIG. 1. Schematic diagram of a shock wave.

Let subscripts 1 and 2 in Fig. 1 denote values at large distances upstream ($x\to-\infty$) and downstream ($x\to\infty$) of the shock front, with $\mathbf{u}=[v(x),0,0]$ and ρ and T be functions only of x. In the frame comoving with the shock front, we have $\partial_t = 0$. Upon integrating Eq. (2.1) to Eq. (2.3) from a uniform upstream state to an arbitrary position x in the shock, we obtain

$$\rho v = \rho_1 v_1, \tag{3.1}$$

$$p + \rho v^2 + \pi_{xx} = p_1 + \rho_1 v_1^2, \tag{3.2}$$

$$\rho v(c_v T + \tfrac{1}{2}v^2) + pv + v\pi_{xx} + q_x = \rho_1 v_1(c_v T_1 + \tfrac{1}{2}v_1^2) + p_1 v_1, \tag{3.3}$$

where $c_v = \frac{3}{2}R$, π_{xx} is the $\hat{x}\hat{x}$ component of the viscous stress tensor given by Eq. (2.4) and q_x is the $\hat{x}$ component of the heat current given by Eq. (2.8). The simple forms of the right sides of these equations result from vanishing of the derivatives of the fluid variables far from the shock.

From Eq. (3.1), we can express ρ in terms of v:

$$\rho = \frac{\rho_1 v_1}{v}. \tag{3.4}$$

Combining Eqs. (3.4) with (3.2) and (3.3) leads to

$$\pi_{xx} = R\rho_1 v_1\left(\frac{T_1}{v_1} - \frac{T}{v}\right) + \rho_1 v_1(v_1 - v), \tag{3.5}$$

$$q_x = \tfrac{3}{2}R\rho_1 v_1(T_1 - T) + p_1(v_1 - v) + \tfrac{1}{2}\rho_1 v_1(v_1 - v)^2. \tag{3.6}$$

We nondimensionlize these equations using v_1 as the unit of speed, T_1 as unit of temperature, and the mean free path at upstream infinity λ_1 as the unit of length. Then, we introduce the nondimensional quantities $X = x/\lambda_1$, $w(X) = v/v_1$, $\theta(X) = T/T_1$ and

$$\varpi(X) = \frac{\pi_{xx}}{p_1} \tag{3.7a}$$

and

$$q(X) = \frac{q_x}{p_1 v_1}. \tag{3.7b}$$

The equations become

$$\varpi = 1 - \frac{\theta}{w} + \frac{5}{3} M_1^2 (1-w), \tag{3.8}$$

$$\frac{2q}{3} = 1 - \theta + \frac{2}{3}(1-w) + \frac{5}{9} M_1^2 (1-w)^2, \tag{3.9}$$

where

$$M_1 = \frac{v_1}{c_1}, \qquad \text{with} \qquad c_1 = \sqrt{\gamma R T_1}$$

and $\gamma = 5/3$.

We see from Eq. (2.6) that the viscosity is $\mu = \tau p$, where τ is the mean flight time of the particles. Here, we adopt the simplest form of the relaxation model, namely, that with constant τ. Then, we follow Gilbarg and Paolucci [16] and take

$$\mu = \frac{\lambda_1 p_1}{\sqrt{2RT_1}} s, \tag{3.10}$$

where s is a parameter that is adjusted according to the nature of the constituent particles. For argon, $s = 0.816$ has often been used [2], but Kestin *et al.* [17] suggested that $s = 0.64$ is a better value for argon. We shall adopt the latter, more recent value in these computations. As to the conductivity, the relaxation model gives $\eta = \frac{5}{2}\mu RT$ but, when the Boltzmann collision term is used, we obtain a slightly different value that is in better agreement with experiment. Because the difference results from the atomic model rather than fluid-dynamical issues, we shall adopt the formula $\eta = 15\mu RT/4$ to remove the effects of the inaccuracy of the atomic model.

To these formulas we adjoin the the closure relations (2.4) and (2.8), that may be rewritten in nondimensional form as

$$\varpi = -\sqrt{\frac{5}{6}} M_1 s \left(2w' + w \frac{\theta'}{\theta} \right) \tag{3.11}$$

$$q = -\frac{3}{2}\sqrt{\frac{5}{6}} \frac{s}{M_1} \left(2\theta' + \frac{10}{9} M_1^2 w w' - \theta \frac{w'}{w} \right), \tag{3.12}$$

where the primes indicate differentiation with respect to X.

Upon combining Eqs. (3.11) and (3.12) with Eqs. (3.8) and (3.9), we obtain the following:

$$-\sqrt{\frac{5}{6}} M_1 s \left(2w' + w \frac{\theta'}{\theta} \right) = 1 - \frac{\theta}{w} + \frac{5}{3} M_1^2 (1-w), \tag{3.13}$$

$$-\frac{3}{2}\sqrt{\frac{5}{6}} \frac{s}{M_1} \left(2\theta' + \frac{10}{9} M_1^2 w w' - \theta \frac{w'}{w} \right) = 1 - \theta + \frac{2}{3}(1-w) + \frac{5}{9} M_1^2 (1-w)^2. \tag{3.14}$$

For comparison, we also write the equations that determine the shock structure from the Navier-Stokes equations:

$$-\frac{4}{3}\sqrt{\frac{5}{6}} M_1 s w' = 1 - \frac{\theta}{w} + \frac{5}{3} M_1^2 (1-w), \tag{3.15}$$

$$-\frac{3}{2}\sqrt{\frac{5}{6}} \frac{s}{M_1} \theta' = 1 - \theta + \frac{2}{3}(1-w) + \frac{5}{9} M_1^2 (1-w)^2. \tag{3.16}$$

B. Critical Mach number

Before carrying out numerical integration of Eqs. (3.13) and (3.14), we examine them in order to draw some general conclusions. First, we observe that, since the x derivatives of w and θ vanish far upstream and downstream, the right sides of Eqs. (3.13) and (3.14) [as well as those of Eqs. (3.15) and (3.16)] must vanish there. These conditions provide two simultaneous equations which are readily solved for the fixed points $(w_1, \theta_1) = (1,1)$ and

$$(w_2, \theta_2) = \left(\frac{M_1^2 + 3}{4M_1^2}, \frac{5M_1^4 + 14M_1^2 - 3}{16M_1^2} \right).$$

Our aim is to find solutions that connect the two fixed points. However, although the fixed points may occur only at the locations in the (w, θ) plane just found, those locations need not be fixed points: the left sides of Eqs. (3.13) and (3.14) may vanish when the determinant of the matrix of the coefficients of the derivatives vanishes. This is seen when we write the equations in the form

$$\mathcal{M} \begin{pmatrix} w' \\ \theta' \end{pmatrix} = -\frac{1}{s}\sqrt{\frac{6}{5}} \begin{pmatrix} \varpi / M_1 \\ M_1 q \end{pmatrix}, \tag{3.17}$$

where

$$\mathcal{M} = \begin{pmatrix} 2 & w/\theta \\ \xi w - \theta / w & 2 \end{pmatrix}, \tag{3.18}$$

with $\xi = 10M_1^2/9$.

If we can solve Eqs. (3.17) and (3.18) to obtain explicit expressions for the derivatives, we can then solve the coupled first-order ordinary differential equations to find solutions connecting the fixed points. This is possible if the determinant of $\mathcal{M}$ does not vanish. The critical condition is then obtained by setting the determinant to zero, a step that leads to the relation

$$\theta = \frac{2}{9} M_1^2 w^2. \tag{3.19}$$

At upstream infinity, we have $(w, \theta) = (1,1)$ and this leads to the critical value $M_1^c = 3/\sqrt{2} \approx 2.12$. We cannot solve for the derivatives when $M_1 > M_1^c$.

When the upstream flow speed is large enough to make the Mach number exceed the critical Mach number M_1^c, D changes its sign. If this leads to either $D_\omega / D > 0$ or $D_\theta / D < 0$ far upstream, it becomes impossible to match the downstream values with a monotonic solution. This happens for any hyperbolic system, as is commonly seen in moment for-

malisms [9] and was first noticed in the study of Grad's 13-moment method. Interestingly, it is numerically verified [9,18] that only when the largest upstream critical Mach number is surpassed does this happen.

In moment methods, as more and more moments are included, the largest critical Mach number increases, and this relaxes the constraints on the application to shock study with the moment method. It will be of interest to see whether higher order terms in our approach will produce a similar amelioration. Still, it is worth noting that the constraints on the Mach number are not due to the expansion scheme, but to the nature of the relaxational model. In a subsequent paper, we shall show that, when a classical Boltzmann integral is used in place of the relaxation term, the constraints on the Mach number are removed. However, physically, information speed cannot be infinite, which indicates that the final version of hydrodynamics must be of a hyperbolic nature.

IV. SHOCK STRUCTURE

To find the structures of shock waves in the continuum limit, we integrated Eqs. (3.13) and (3.14) for different Mach numbers in the range allowed. Here in Sec. IV, we compare the results with those obtained with the conventional Navier–Stokes equations and also with experimental data. To facilitate such comparisons, we note that the differences between our stress tensor and heat flux and those in the conventional fluid dynamical equations reside in the quantities,

$$\Delta \mathsf{P} = -\mu(\mathcal{D}_0 \ln T + \tfrac{2}{3}\boldsymbol{\nabla}\cdot\mathbf{u})\mathsf{I}, \tag{4.1}$$

$$\Delta \mathbf{Q} = -\left(\eta \boldsymbol{\nabla} \ln(\rho T) + \frac{5}{2}\mu \frac{D\mathbf{u}}{Dt}\right). \tag{4.2}$$

These are extra terms in our version for the stress tensor and heat flux compared to in the usual Navier-Stokes (NS) form. In one-dimensional flow with $\hat{\mathbf{x}}$ as the unit vector in the x direction, we may write these as

$$\Delta \mathbf{P} = \Delta P \hat{x}\hat{x}, \tag{4.3}$$

$$\Delta \mathbf{Q} = \Delta Q \hat{x}, \tag{4.4}$$

with ΔP and ΔQ given by

$$\Delta P = -\mu\left(\frac{D \ln T}{Dt} + \frac{2}{3}v'\right), \tag{4.5}$$

$$\Delta Q = -\left(\eta[\ln(\rho T)]' + \frac{5}{2}\frac{Dv}{Dt}\right). \tag{4.6}$$

We may use the upstream quantities to write these formulas in nondimensional form as

$$dP \equiv \frac{\Delta P}{p_1} = -\sqrt{\frac{\gamma}{2}} s M_1 \left(\frac{\theta'}{\theta} + \frac{2}{3}\omega'\right), \tag{4.7}$$

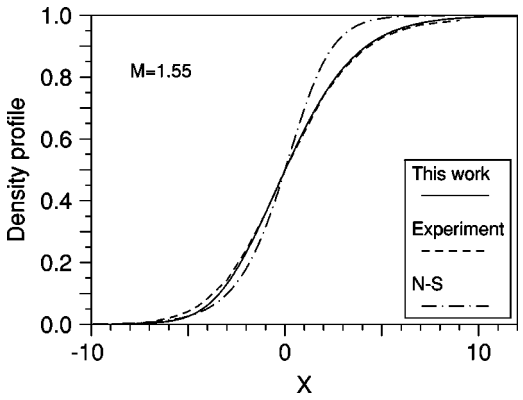

FIG. 2. Comparison of the density profile with Mach number $M = 1.55$.

$$dQ \equiv \frac{2\Delta Q}{3p_1 v_1} = -\frac{2}{3}\sqrt{\frac{\gamma}{2}} s M_1 \left[\frac{15\theta}{4\gamma M_1^2}\left(\frac{\omega}{\omega'} - \frac{\theta'}{\theta}\right) + \frac{5}{2}\omega\omega'\right]. \tag{4.8}$$

Neither of these is included in the usual derivations of the NS equations. This neglect is not advisable when the Knudsen number is not small as we confirm with the following results.

Figure 2 shows a comparison of the theoretical density profiles (for $M_1 = 1.55$) with the experimental measurement given by Alsmeyer [19]. We have computed and included in Fig. 2 profiles for the NS equations as well as our own. We see that the present theory agrees better with experiment. We make a similar comparison for temperature in Fig. 3, but this time make the comparison with results of a Monte Carlo simulation result [19] in place of the experiment. Again the fit of our theory is quite good whereas that for the Navier–Stokes equations is less so.

Next we examine some properties that are often used by experimentalists to characterize shock waves. The most revealing of these is the inverse thickness,

$$\delta^{-1} = \frac{\rho_m'}{\rho_2 - \rho_1}, \tag{4.9}$$

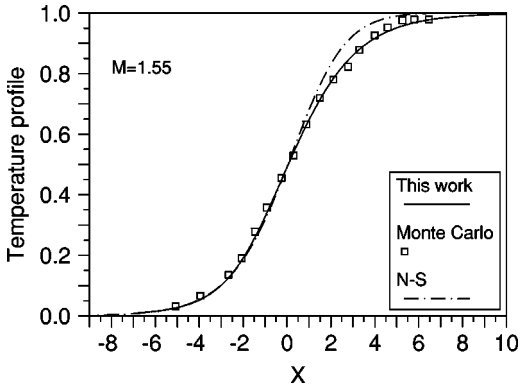

FIG. 3. Comparison of the temperature profile with Mach number $M = 1.55$.

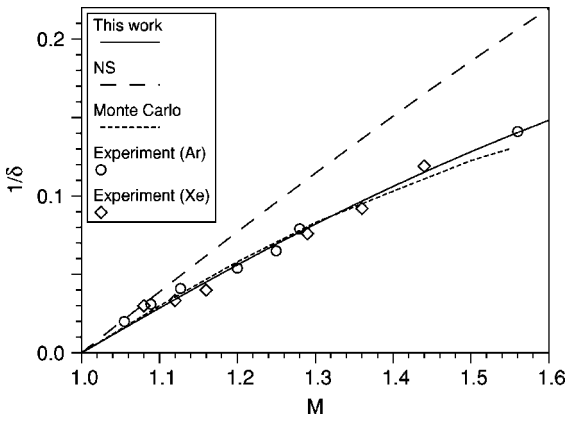

FIG. 4. Inverse thickness.

where ρ_m' is the maximum value of the gradient of density profile, and, as before, ρ_1 and ρ_2 are the upstream and downstream densities, respectively. Next, we have the asymmetry parameter [5],

$$A_s=\frac{\int_{\rho_a}^{\rho_2}\rho dx}{\int_{\rho_1}^{\rho_a}\rho dx}, \tag{4.10}$$

with $\rho_a=\frac{1}{2}(\rho_2-\rho_1)$. Finally, the temperature–density separation $\Delta_{\rho T}$ is defined as the distance between the medium value points of temperature and density.

Figure 4 shows the inverse thickness versus the Mach number. Experimental data for argon and xenon are also shown. While the fit from our equations is good, the results also show a known failing of the NS equations, namely, they predict shock structures that are narrower than those seen experimentally. This difference is corrected by the extra terms in our equations. That is, improved theoretical profiles result from the inclusion of the nonzero dP and dQ, as we see from the plots in Figs. 5 and 6 that show the scaled density, temperature, and velocity, together with dP and dQ for Mach numbers $M_1=1.5$ and 2.0, respectively. The analogous results from the Navier-Stokes equations were computed and plotted for comparison.

Our estimates of the local dissipation show that the net effect on the shock structure caused by dP and dQ increases monotonically from the downstream to the upstream, which tends to lower the gradients of the thermodynamical variables and results in wider shocks. Such effects become more noticeable when Mach number is larger, as is seen in Figs. 5 and 6. We can see that, with a increase of the Mach number, the additional terms from our modified procedure become more and more significant and that their effects are no longer negligible at a moderate Mach number. They produce extra dissipation, which makes the gradients of the thermodynamic variables smoother in doing and so widen the shock.

As for the asymmetry parameter, in the case of $M_1=2.0$, the NS equations give $A_s=1.25$, while our modification of them gives $A_s=0.83$, which is closer to the experimental value of 0.93. Aside from the quantitative improvement, the modified version also becomes qualitatively consistent with

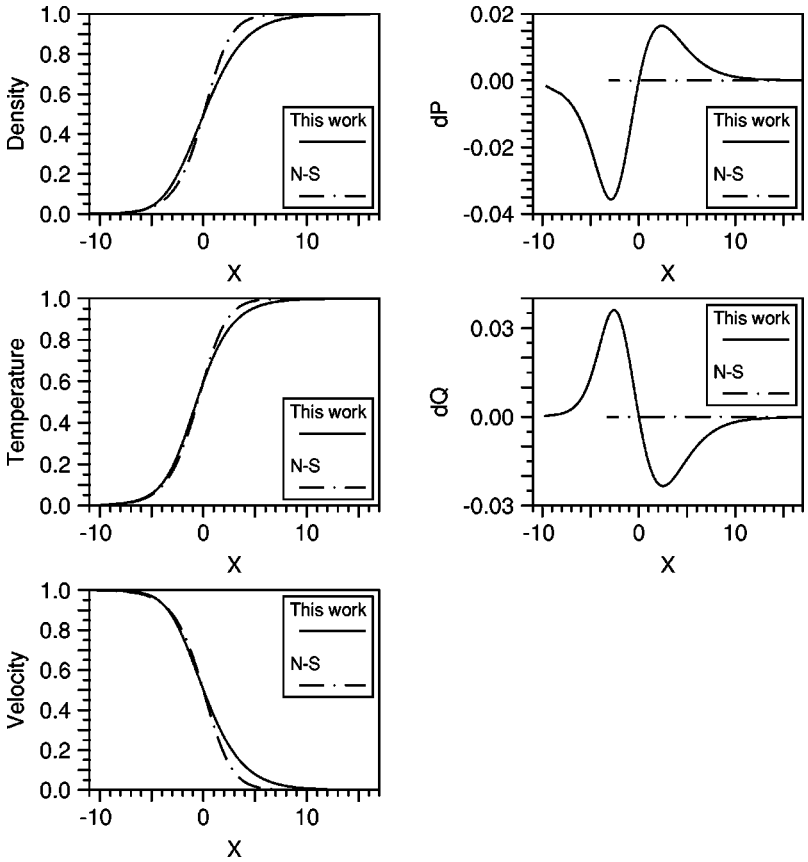

FIG. 5. Density, temperature, velocity, and dP and dQ profiles with Mach number $M=1.5$.

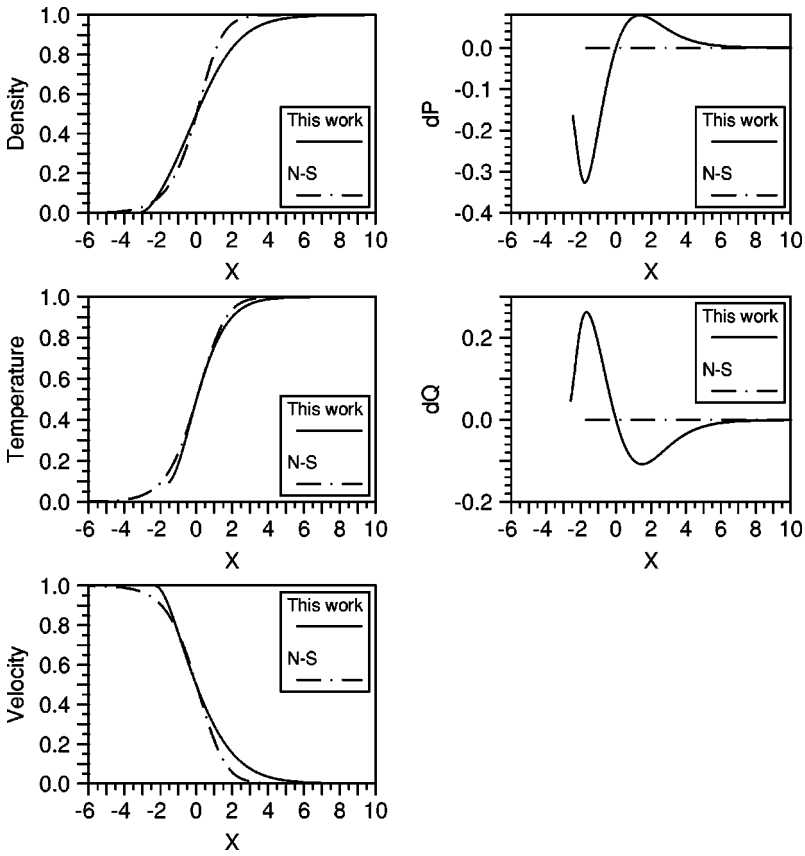

FIG. 6. Density, temperature, velocity, and dP and dQ profiles with Mach number $M=2.0$.

the experiment, that is, A_s should be smaller than unity. For Mach number $M_1=2.0$, the NS equations lead to a temperature–density separation of 1.04, whereas the modified version leads to one of 1.67 and the experimental data for argon is one of 1.50 [5].

V. CONCLUSION

We have seen that modification of the Hilbert expansion described in paper I [12] leads to a good representation of shock structures found experimentally for Mach numbers between 1.0 and 2.12. The results are distinctly better than those obtained from the Navier–Stokes equations derived with the standard Chapman–Enskog procedure. The agreement with numerical results from the kinetic theory obtained by Monte Carlo simulation is also good.

The structures calculated here are steady. However, in the study of rapid variations produced by high-frequency sound wave propagation in Ref. [13], the modified fluid equations produced results that were in good agreement with experiment for the speed of propagation of the waves uniformly for all Knudsen numbers.

In our derivations, we did not follow Chapman and Enskog in requiring that the gradient terms be small. The results reveal that this is an effective method that gives equations capable of describing equations that are valid for processes far from equilibrium. In a later paper we shall apply them to the derivation of fluid equations from the Boltzmann equation. In this way we obtain very similar continuum equations but avoid the problem of the existence of a critical Mach number (see Sec. III B).

[1] V. Galkin and S. Shavaliev, Fluid Dyn. **33**, 469 (1998).
[2] S. Chapman and T. G. Cowling, *The Mathematical Theory of Non-Uniform Gases*, 3rd ed. (Cambridge University Press, Cambridge, 1970).
[3] H. Grad, Phys. Fluids **6**, 147 (1963).
[4] R.M.X. Zhong and R. Chapman, AIAA J. **31**, 1036 (1993).
[5] K. A. Fiscko and D. R. Chapman, in *Progress in Astronautics and Aeronautics, AIAA*, edited by E. P. Muntz, D. P. Weaver, and D. H. Campbell (American Institute of Aeronautics and Astronautics, Washington, DC, 1989), Vol. 118, p. 374.
[6] L. C. Woods, *An Introduction to Kinetic Theory of Gases and Magnetoplasma* (Oxford University Press, Oxford, UK, 1993).
[7] Y.L. Klimontovich, Theor. Mat. Phys. **92**, 909 (1992).
[8] H. Grad, Commun. Pure Appl. Math. **2**, 331 (1949).
[9] I. Müller and T. Ruggeri, *Rational Extended Thermodynamics*, Springer Tracts in Natural Philosophy, 2nd ed. (Springer, New York, 1998), Vol. 37.
[10] R. Myong, Phys. Fluids **11**, 2788 (1999).
[11] K.H. Prendergast and K. Xu, J. Comput. Phys. **109**, 53 (1993).
[12] X. Chen, H. Rao, and E.A. Spiegel, Phys. Rev. E **64**, 046308 (2001).
[13] X. Chen, H. Rao, and E.A. Spiegel, Phys. Rev. E **64**, 046309

(2001).
[14] X. Chen, Ph.D. thesis, Columbia University, New York, NY, 2000.
[15] X. Chen, H. Rao, and E.A. Spiegel, Phys. Lett. A **271**, 87 (2000).
[16] D. Gilbarg and D. Paolucci, J. Rat. Mech. Anal. **2**, 617 (1953).
[17] J. Kestin *et al.*, J. Phys. Chem. Ref. Data **13**, 229 (1984).
[18] W. Weiss, Phys. Rev. E **52**, 5760 (1995).
[19] H. Alsmeyer, J. Fluid Mech. **74**, 497 (1976).